

# Development of a Whole-Cell Biocatalyst/Biosensor by Display of Multiple Heterologous Proteins on the *Escherichia coli* Cell Surface for the Detoxification and Detection of Organophosphates

Ruihua Liu,<sup>†,||</sup> Chao Yang,<sup>‡,||</sup> Yingming Xu,<sup>§</sup> Ping Xu,<sup>\*,#</sup> Hong Jiang,<sup>⊥</sup> and Chuanling Qiao<sup>\*,⊥</sup>

<sup>†</sup>College of Pharmacy and Tianjin Key Laboratory of Molecular Drug Research, Nankai University, Tianjin 300071, China

<sup>‡</sup>Key Laboratory of Molecular Microbiology and Technology for Ministry of Education, College of Life Sciences, Nankai University, Tianjin 300071, China

<sup>§</sup>Tianjin Key Laboratory of Agro-environment and Agro-product Safety, Institute of Agro-Environmental Protection, Ministry of Agriculture, Tianjin 300191, China

<sup>#</sup>State Key Laboratory of Microbial Metabolism, Shanghai Jiao Tong University, Shanghai 200240, China

<sup>⊥</sup>State Key Laboratory of Integrated Management of Pest Insects and Rodents, Institute of Zoology, Chinese Academy of Sciences, Beijing 100101, China

## **S** Supporting Information

**ABSTRACT:** This paper reports the codisplay of organophosphorus hydrolase (OPH) and methyl parathion hydrolase (MPH)–green fluorescent protein (GFP) fusion on the cell surface of *Escherichia coli* using the truncated ice nucleation protein (INPNC) and Lpp–OmpA as the anchoring motifs. The surface localization of both OPH and MPH–GFP was demonstrated by cell fractionation, Western blot analysis, protease accessibility experiment, and immunofluorescence microscopy. Anchorage of the foreign proteins on the outer membrane neither inhibits cell growth nor affects cell viability. The recombinant strain can be used as a whole-cell biocatalyst and showed a broader substrate range than strains expressing either OPH or MPH. A mixture of six organophosphorus pesticides (OPs) (0.2 mM each) could be degraded completely within 5 h. The broader substrate specificity in combination with the rapid degradation rate makes the recombinant strain a promising candidate for detoxification of OPs. The fluorescence of surface-displayed GFP is very sensitive to environmental pH change. Because hydrolysis of OPs by OPH or MPH generates protons, the recombinant *E. coli* could be used as a whole-cell biosensor for the rapid detection of OPs by evaluating fluorescence changes as a function of OP concentrations.

**KEYWORDS:** surface display, organophosphorus hydrolase, methyl parathion hydrolase, green fluorescent protein

## **I** INTRODUCTION

Organophosphorus pesticides (OPs) have been used extensively all over the world for crop protection, accounting for ~38% of the total pesticides used globally.<sup>1</sup> OPs are acetylcholinesterase (AChE) inhibitors, leading to loss of nerve functions and even death.<sup>2</sup> Unintentional pesticide exposure results in 1 million to 3 million poisonings annually worldwide. Due to the widespread use of OPs, their residues and metabolites are accumulated in soil, water, and food.

Bacterial enzymatic detoxification of OPs has attracted considerable interest, because it is economical and effective. The extensively studied organophosphorus hydrolases (OPH) were originally found in two parathion-degrading soil bacteria: *Flavobacterium* sp. strain ATCC 27551 from the Philippines and *Pseudomonas diminuta* MG from the United States.<sup>3,4</sup> OPH are zinc-containing homodimeric phosphotriesterases that can hydrolyze parathion and a variety of other OPs. Hydrolysis of OPs by OPH reduces their toxicity by several orders of magnitude.<sup>5</sup> However, the rates of hydrolysis of some OPs vary dramatically because of the structural diversity of individual members of the family of OPs. For example, methyl parathion and chlorpyrifos are hydrolyzed by OPH 30- and 1200-fold more slowly compared to the preferred substrate, paraoxon.<sup>6,7</sup>

Methyl parathion hydrolase (MPH) found in methyl parathion-degrading *Plesiomonas* sp. strain M6 isolated in China is a novel OP hydrolase reported.<sup>8</sup> The amino acid sequence of the MPH shows no homology with that of the OPH. Importantly, the OPH and MPH have complementary substrate specificity toward OPs.

The use of purified OPH or MPH for detoxification has always been limited by the cost of purification and stability of the enzyme. Whole-cell detoxification is an alternative strategy to purified enzymes; however, it is limited by the transport barrier of OPs across the cell membrane. A clever solution is the anchorage of OP hydrolases on the cell surface. So far, OPH or MPH has been displayed on the cell surface of *Escherichia coli*,<sup>9</sup> *Moraxella* sp.,<sup>10</sup> *Pseudomonas putida*,<sup>11,12</sup> and *Saccharomyces cerevisiae*<sup>13</sup> when fused to surface-anchoring motifs.

Several surface-anchoring motifs, including Lpp–OmpA chimera, INP, and autotransporter, have been widely used to display proteins on the surface of Gram-negative bacteria.<sup>14,15</sup>

**Received:** April 28, 2013

**Accepted:** July 22, 2013

**Published:** July 22, 2013

Table 1. Strains, Plasmids, and Primers Used in This Study

strain, plasmid, or primer	description	source or reference
<i>E. coli</i> strains		
XL1-Blue	<i>recA1 endA1 gyrA96 thi-1 hsdR17</i> (r <sub>K</sub> -m <sub>K</sub> <sup>+</sup> ) <i>supE44 relA1 lac</i> (F' <i>proAB lacI</i> <sup>q</sup> ZΔM15 Tn10 [Tet <sup>r</sup> ])	Stratagene
DH5α	<i>supE44 ΔlacU169</i> (φ80 <i>lacZ</i> ΔM15) <i>recA1 endA1 hsdR17</i> (r <sub>K</sub> -m <sub>K</sub> <sup>+</sup> ) <i>thi-1 gyrA relA1 F<sup>-</sup> Δ(lacZYA-argF)</i>	Tiagen
plasmids		
pOP131	gene source of Lpp–OmpA fusion	9
pMDQ	source of <i>mpd</i> gene	27
pEGFP-N3	source of <i>gfp</i> gene	23
pUC18	expression vector, <i>lac</i> promoter, Ap <sup>r</sup>	TaKaRa
pLMG18	pUC18 derivative, vector for expressing Lpp–OmpA–MPH–GFP on the cell surface	this study
pVLT33	<i>E. coli</i> – <i>Pseudomonas</i> shuttle vector, <i>oriT</i> , RSF1010, <i>oriV lacIq</i> , <i>tac</i> promoter, Km <sup>r</sup>	25
pPNC033	pVLT33 derivative, surface expression vector coding for INPNC–OPH fusion	10
pCPO	pVLT33 derivative, control plasmid for expressing a cytosolic OPH	26
pMG18	pUC18 derivative, control plasmid for expressing a cytosolic MPH–GFP fusion	this study
primers		
P1	<u>GAATTCCTCTAGAGGGTATTAATAATGAAAGCTACTAAACTGGTA</u>	this study
P2	<u>GGATCCGTTGTCGGACGAGTGCCGAT</u>	this study
P3	<u>GGATCCATGGCCGCACCGCAGGTG</u>	this study
P4	<u>CTGCAGCTTGGGGTTGACGACCG</u>	this study
P5	<u>CTGCAGATGGTGAGCAAGGGC</u>	this study
P6	<u>AAGCTTACTTGTACAGCTCGTCCA</u>	this study
P7	<u>GAATTCCTCTAGAGGGTATTAATAATGGCCGCACCGCAGGTG</u>	this study

The Lpp–OmpA chimera consists of the signal sequence and the first nine N-terminal amino acids of the major *E. coli* lipoprotein (Lpp) joined to a transmembrane domain (amino acids 46–159) from outer membrane protein A (OmpA).<sup>16</sup> The ice nucleation protein (INP), an outer membrane protein of *P. syringae*, capable of inducing ice-crystal formation in supercooled water, consists of an N-terminal region interacting with the phospholipid moiety of the outer membrane, a central repeat region involved in ice nucleation and a C-terminal highly hydrophilic region exposed to the cell surface.<sup>17,18</sup>

Green fluorescent protein (GFP) is used widely as a fluorescent marker for monitoring gene expression and protein localization.<sup>19,20</sup> The fluorescence of GFP is very sensitive to pH in vitro and in vivo, and GFP fluorescence responds rapidly and reversibly to pH changes.<sup>21</sup> Numerous GFP variants with different pH sensitivities have been obtained, and GFP variants display greater pH sensitivity than wild-type GFP. Wild-type GFP is quenched by acidic pH values, and several of the GFP mutants are more acid sensitive than wild-type GFP. For example, 50% of the fluorescence of enhanced GFP (EGFP) was quenched at pH 5.5.<sup>22,23</sup>

In this study, we aimed to construct a whole-cell biocatalyst/biosensor by coexpressing OPH and MPH–GFP fusion protein on the cell surface of *E. coli*. The recombinant *E. coli* showed a broader substrate specificity toward OPs and could be used for OP detection by evaluating fluorescence changes as a function of OP concentrations.

## MATERIALS AND METHODS

**Bacterial Strains, Plasmids, and Culture Conditions.** *E. coli* XL1-Blue was used as a host for codisplay of OPH, MPH, and GFP. *E. coli* strains bearing plasmids were grown in Luria–Bertani (LB) medium<sup>24</sup> supplemented with ampicillin (100 μg/mL) and/or kanamycin (20 μg/mL) at 250 rpm and 37 °C. When the *E. coli* culture reached an OD<sub>600</sub> of 0.5, 0.2 mM IPTG was added to induce protein expression for 24 h at 30 °C.

A surface expression vector, pPNC033,<sup>10</sup> coding for INPNC–OPH was used to target OPH onto the cell surface. The *inpnc–opd* fragment was PCR amplified from pINCOP and subcloned into *EcoRI/HindIII*-

digested pVLT33,<sup>25</sup> an *E. coli*–*Pseudomonas* shuttle vector, to generate pPNC033. Plasmid pCPO<sup>26</sup> was used for the production of a cytosolic OPH.

The *lpp–ompA* fusion gene was PCR amplified from plasmid pOP131<sup>9</sup> using primers P1 and P2. The PCR product was digested with *EcoRI* and *BamHI* and then ligated into similarly digested pUC18 to generate pL18. The *mpd* gene was PCR amplified from plasmid pMDQ<sup>27</sup> using primers P3 and P4. The PCR product was digested with *BamHI* and *PstI* and then ligated into similarly digested pL18 to generate pLM18. The *gfp* gene was PCR-amplified from plasmid pEGFP-N3<sup>23</sup> using primers P5 and P6. The PCR product was digested with *PstI* and *HindIII* and then ligated into similarly digested pLM18 to generate pLMG18.

To construct a control plasmid for expressing the MPH–GFP fusion protein in the cytoplasm, the *mpd–gfp* fusion gene was PCR-amplified from plasmid pLMG18 using primers P7 and P6. The PCR product was digested with *EcoRI* and *HindIII* and then ligated into similarly digested pUC18 to generate pMG18. All plasmid constructions were verified by DNA sequence analysis. Transformation of plasmid into *E. coli* was carried out using the CaCl<sub>2</sub> method.<sup>24</sup> All strains, plasmids, and primers used in this study are listed in Table 1.

**SDS-PAGE and Western Blot Analysis.** To verify the surface localization of INPNC–OPH and Lpp–OmpA–MPH–GFP fusion protein, cells were fractionated to yield soluble fraction and outer membrane fraction by differential centrifugation.<sup>28</sup> Protein samples were analyzed on 10% (w/v) SDS-PAGE,<sup>24</sup> followed by electrophoretic transfer to a nitrocellulose membrane (Millipore) with transfer buffer (25 mM Tris, 192 mM glycine, 10% methanol) by using Trans-Plot SD Cell (Bio-Rad). Blotted membrane was blocked in TBST buffer (20 mM Tris-HCl, pH 7.5, 150 mM NaCl, 0.05% Tween-20) with 5% (w/v) skim milk. The membrane was then incubated with rabbit anti-GFP polyclonal antibody (Abcam) or anti-OPH serum<sup>10</sup> at a dilution of 1:500 and probed with goat anti-rabbit IgG secondary antibody conjugated with alkaline phosphatase (1:1000) (Promega). Both antibodies were added in TBST/5% skim milk and incubated at room temperature for 2 h. The membrane was then stained with FAST BCIP/NBT (Sigma) kit for visualizing antigen–antibody conjugates.

**Immunofluorescence Microscopy.** Cells were harvested and resuspended in PBS containing 3% BSA (OD<sub>600</sub> = 0.5) for blocking at 30 °C for 1 h. Then cells were incubated with anti-GFP antibody or anti-OPH serum diluted (1:500) in PBS at 30 °C for 2 h. After washing with PBS buffer, the cell–antibody complex was incubated

with goat anti-rabbit IgG conjugated with rhodamine (Invitrogen) at a dilution of 1:50 at 30 °C for 1.5 h. Finally, cells were washed with PBS and examined by using a fluorescence microscope (Olympus).

**Assays for the OP Hydrolase Activity.** The activities of whole cells expressing OPH and MPH were measured by using six OPs as the substrates. Hydrolysis of paraoxon, parathion, and methyl parathion was measured spectrophotometrically by monitoring the formation of *p*-nitrophenol at 405 nm ( $\epsilon_{405} = 17700 \text{ M}^{-1} \text{ cm}^{-1}$ ) with a Beckman DU800 spectrophotometer.<sup>9</sup> Hydrolysis of fenitrothion was measured by quantifying the production of 3-methyl-4-nitrophenol at 358 nm ( $\epsilon_{358} = 18700 \text{ M}^{-1} \text{ cm}^{-1}$ ). Hydrolysis of chlorpyrifos and diazinon was measured by using an Agilent 1100 series HPLC and a HP 5890 II GC, respectively.<sup>27</sup> The OPH activity assay was carried out at 30 °C in 100 mM phosphate buffer (pH 7.4) supplemented with 0.2 mM substrate and 100  $\mu\text{L}$  of cells ( $\text{OD}_{600} = 1.0$ ). Activities were expressed in units (1  $\mu\text{mol}$  of substrate hydrolyzed per minute) per  $\text{OD}_{600}$  whole cells.

**Measurement of Whole-Cell Fluorescence.** The whole-cell GFP fluorescence was determined using a fluorescence spectrophotometer (F-4500; Hitachi, Japan) as described previously.<sup>29</sup>

**Protease Accessibility Assay.** The IPTG-induced cells were resuspended in PBS buffer (pH 7.5) and adjusted to an  $\text{OD}_{600}$  of 10. Pronase (4 units/mg, Sigma) was added to a final concentration of 2 mg/mL. The cell suspensions were incubated at 37 °C for 3 h. Pronase-treated and untreated cells were assayed for OPH activity and GFP fluorescence.

**Stability Study of Resting Cultures.** For outer membrane integrity analysis, the OPH activity of the resting-cell suspension was determined each day over 2 weeks.<sup>29</sup>

**Biodegradation of OPs by Recombinant *E. coli*.** The recombinant *E. coli* cells were harvested after 24 h of induction and then washed with 100 mM phosphate buffer (pH 7.4) twice and resuspended ( $\text{OD}_{600} = 1.0$ ) in the same buffer. The biodegradation experiments were carried out using a mixture of paraoxon, parathion, methyl parathion, fenitrothion, diazinon, and chlorpyrifos. All OPs were added to the cell suspension at an initial concentration of 0.2 mM. Samples were incubated at 30 °C on a shaker at 150 rpm and then taken at regular time intervals. The remaining pesticide in the suspension was extracted with trichloromethane, and the extracts were then dried over anhydrous  $\text{Na}_2\text{SO}_4$ . Samples of 1  $\mu\text{L}$  (diluted if necessary) were analyzed by using a HP 5890 II GC equipped with a NPD detector and a capillary HP-1 column. The GC detection conditions are described in Yang et al.<sup>27</sup> The concentration of pesticides was determined by comparing the peak area of the samples to a standard curve.

**Correlation of OP Concentration with GFP Fluorescence.** For the pH sensitivity tests of the GFP fluorescence, cells were suspended ( $\text{OD}_{600} = 1.0$ ) in different phosphate buffers with a pH range of 4–8. The fluorescence intensity of GFP was measured with the cell suspension by using a fluorescence spectrophotometer as described above. To investigate the correlation of OP concentration with GFP fluorescence, the fluorescence intensity was measured using a PBS buffer (pH 7.5) supplemented with 0.02–0.2 mM parathion or methyl parathion and 100  $\mu\text{L}$  of cells ( $\text{OD}_{600} = 1.0$ ).

## RESULTS AND DISCUSSION

**Surface Localization of OPH and MPH–GFP Fusion on *E. coli*.** To minimize direct competition for the same translocation machinery, in this study, two different anchoring motifs (truncated INP and Lpp–OmpA chimera) were employed for the targeting of OPH and MPH–GFP fusion onto the *E. coli* cell surface. For this purpose, a pVLT33-based vector, pPNC033, coding for INPNC–OPH fusion, and a pUC18-based vector, pLMG18, coding for Lpp–OmpA–MPH–GFP fusion, were cotransformed (1  $\mu\text{L}$  of each) into *E. coli*.

Plasmid incompatibility is often a concern when more than one vector is propagated within a system. Plasmids sharing the

same origin of replication (*ori*) cannot stably coexist in a host cell.<sup>30</sup> When a dual plasmid system is used, one strategy is to begin with two compatible vectors. pUC18 contains a pBR322 *ori*, an ampicillin resistance marker, and a *lac* promoter, whereas pVLT33 contains an RSF *ori*, a kanamycin resistance marker, and a *tac* promoter.<sup>25</sup> Consequently, pUC18 and pVLT33 can stably coexist in *E. coli* during cell growth.

Production of the INPNC–OPH fusion was demonstrated by Western blotting with anti-OPH serum. A band corresponding to INPNC–OPH at 82 kDa was detected in whole-cell lysates (Figure 1A, lane 4). However, no target protein was

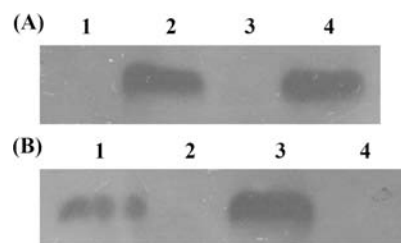


**Figure 1.** Western blot analysis for subcellular localization of INPNC–OPH and Lpp–OmpA–MPH–GFP fusion protein in *E. coli*. (A) Western blot analysis of different cellular fractions with anti-OPH serum. Lanes: 1, soluble fraction; 2, outer membrane fraction; 3, negative control (*E. coli* carrying pVLT33); 4, whole-cell lysates. (B) Western blot analysis of different cellular fractions with anti-GFP antibody. Lanes: 1, outer membrane fraction; 2, soluble fraction; 3, whole-cell lysates; 4, negative control (*E. coli* carrying pUC18).

detected with the control cells carrying pVLT33. The localization of INPNC–OPH fusion in the outer membrane fraction was also demonstrated by immunoblotting (Figure 1A, lane 2). Expression of the Lpp–OmpA–MPH–GFP fusion was probed by Western blotting with anti-GFP antibody. A band corresponding to Lpp–OmpA–MPH–GFP at 78 kDa was detected in both whole-cell lysates and outer membrane fractions (Figure 1B, lanes 3 and 1, respectively). Assays for the OP hydrolase activity were performed with outer membrane, whole cell, and cell lysate. Over 80% of the activity was detected in the outer membrane fraction. In parallel, >80% of the activity was present on the cell surface as judged from the ratio of whole-cell activity to cell lysate activity (Table 2).

**Table 2.** Percentage of the OP Hydrolases and GFP Displayed on the *E. coli* Cell Surface As Estimated from Protease Treatment, Whole Cell versus Cell Lysate Assays, and Membrane Fractionation Experiments<sup>a</sup>

plasmid	% decrease in activity (FI <sup>b</sup> ) in protease-treated cells	whole-cell activity (as % of cell lysate activity)	% activity (FI) in the outer membrane fraction
pPNC033/pLMG18	82 (81)	84	81 (76)
pCPO/pMG18	7 (6)	6	4 (5)

<sup>a</sup>The OP hydrolase activity was measured with parathion as the substrate. <sup>b</sup>FI, fluorescence intensity.

Protease accessibility assays were performed to ascertain the surface localization of OPH and MPH–GFP fusion. Proteases cannot penetrate the outer membrane and, therefore, only surface-exposed proteins can be degraded by proteases.<sup>9</sup> GFP is resistant to many common proteases but not Pronase, which is a mixture of broad-specificity proteases.<sup>31</sup> After incubation with

Pronase for 3 h, an 81% reduction of the fluorescence intensity was observed in cells carrying pPNCO33/pLMG18, which contrasted with the slight reduction (6%) observed in Pronase-treated control cells carrying pCPO/pMG18. The OP hydrolase activity for Pronase-treated cells decreased by 82%, whereas the activity for Pronase-treated control cells dropped only 7%. The outer membrane samples of Pronase-treated cells were probed with either anti-OPH serum or anti-GFP polyclonal antibody. As expected, no target proteins were detected in the outer membrane fraction because of the degradation of surface-exposed OPH and GFP by Pronase.

Immunolabeling with specific antibodies or antisera is a useful tool to detect surface-exposed proteins.<sup>32</sup> Because antibodies cannot diffuse through the outer membrane, specific interactions should occur only with proteins exposed on the cell surface. To confirm the presence of OPH and MPH–GFP fusion on the cell surface, cells were probed with either anti-OPH serum or anti-GFP polyclonal antibody and then fluorescently stained with rhodamine-labeled IgG antibody. Under a fluorescence microscope, the orange fluorescence was observed on the cells carrying pPNCO33/pLMG18 (data not shown), which indicated that the cell surface was covered with antibody–TRITC complex. In contrast, the control cells carrying pCPO/pMG18 were not immunostained at all. Cells carrying pPNCO33/pLMG18 were incubated for 3 h with Pronase and then immunolabeled with anti-GFP polyclonal antibody and rhodamine-conjugated IgG antibody. As a result, Pronase-treated cells were not immunostained completely, indicating that surface-exposed GFP was removed by Pronase.

Taken together, these results provide strong evidence that the OPH and MPH–GFP fusion was not only codisplayed successfully on the cell surface using the INP and Lpp–OmpA system but also retained the OP hydrolase activity and GFP fluorescence.

**OP Hydrolase Activity and GFP Fluorescence.** Prior to IPTG induction, the OP hydrolase activity was not detected and the fluorescence intensity remained at the original background level. The OP hydrolase activity and fluorescence intensity increased gradually after induction with 0.2 mM IPTG and reached maxima at 24 h (Table 3). In *E. coli*, the outer membrane prevents OPs from interacting with OPH residing within the cell, reducing the overall catalytic efficiency. It was reported that whole cells of *E. coli* displaying OPH degraded parathion and paraoxon 7-fold more rapidly compared to whole cells with an intracellular OPH.<sup>9</sup> In this study, the OP hydrolase activities of whole cells coexpressing OPH and MPH

**Table 3. Time Course of the OP Hydrolase Activity and GFP Fluorescence Intensity of Whole Cell<sup>a</sup>**

time postinduction (h)	OP hydrolase activity (U/OD <sub>600</sub> )	GFP fluorescence intensity
0	nd <sup>b</sup>	31 ± 2
6	0.012 ± 0.002	271 ± 16
12	0.031 ± 0.003	564 ± 20
18	0.116 ± 0.026	634 ± 21
24	0.154 ± 0.032	671 ± 29

<sup>a</sup>Cells harboring pPNCO33 and pLMG18 were incubated at 30 °C for 24 h after induction with 0.2 mM IPTG. Samples were withdrawn at regular time intervals and then measured for the OP hydrolase activity (using parathion as the substrate) and GFP fluorescence intensity of whole cell. The data are mean values ± standard deviations of three replicates. <sup>b</sup>nd, not detected.

(pPNCO33/pLMG18) on the cell surface were 4–6-fold higher than those of whole cells coexpressing OPH and MPH (pCPO/pMG18) intracellularly when using the same amount of cells. The OPH and MPH displayed on the cell surface have free access to extracellular OPs, which enhanced whole-cell catalytic activity.

Directed evolution has been used to generate OPH variants with up to 25- and 700-fold improvement in the hydrolysis of methyl parathion and chlorpyrifos, respectively.<sup>6,7</sup> The obvious question is whether similar success could be achieved with other poor substrates of OPH. Expression of multiple degrading enzymes in a host strain may also be a choice for the acquisition of an enlarged substrate range. An *E. coli* strain capable of simultaneously degrading organophosphorus, carbamate, and pyrethroid classes of pesticides was constructed by coexpressing OPH and carboxylesterase B1.<sup>33</sup> There are 71 commercial OPs that are listed by Tomlin,<sup>34</sup> 33 and 26 of which contain diethyl and dimethyl alkyl groups, respectively. OPH has been shown to lack any hydrolytic activity with numerous dimethyl OPs, whereas MPH shows higher hydrolytic activity for dimethyl OPs.<sup>8,35</sup>

As shown in Table 4, the recombinant strain coexpressing OPH and MPH showed 9.8- and 6.8-fold higher activity for

**Table 4. Whole-Cell Activity of the Recombinant *E. coli* Strains Expressing OPH and/or MPH<sup>a</sup>**

	pPNCO33/ pLMG18	pPNCO33	pLMG18	pCPO/ pMG18
paraoxon	0.281	0.351	0.048	0.046
parathion	0.152	0.178	0.107	0.037
methyl parathion	0.254	0.026	0.315	0.051
fenitrothion	0.102	0.015	0.154	0.021
diazinon	0.005	0.008	nd <sup>b</sup>	0.001
chlorpyrifos	0.016	nd	0.062	0.004

<sup>a</sup>The OP hydrolase activity was assayed with six OPs as the substrate as described under Materials and Methods. Activities were expressed in units (1 μmol of substrate hydrolyzed per minute) per OD<sub>600</sub> whole cells. The data are mean values of three independent experiments. <sup>b</sup>nd, not detected.

methyl parathion and fenitrothion, respectively, compared to a strain expressing OPH. The coexpression strain showed 5.9- and 1.4-fold higher activity for paraoxon and parathion, respectively, compared to a strain expressing MPH. No activity for chlorpyrifos and diazinon was detected with strains expressing OPH or MPH. Compared to previously developed recombinant strains displaying OPH or MPH,<sup>12,26,29</sup> the recombinant strain codisplaying OPH and MPH was endowed with a broader substrate specificity toward OPs.

The protein translocation pathway might be blocked under a high transcription rate, which further causes growth inhibition of cells.<sup>36</sup> In this study, activity and fluorescence under different levels of induction were investigated. As shown in Figure 2a, the highest whole-cell activity was obtained with 0.2 mM IPTG, and further induction resulted in a gradual decline in activity. More IPTG caused declines in activity, probably because of the formation of inclusion body and growth inhibition at increased transcription rates. The fluorescence intensity of GFP increased with increasing concentrations of IPTG (Figure 2b). It is concluded that induction with 0.2 mM IPTG provides an optimal balance between whole-cell activity and fluorescence.

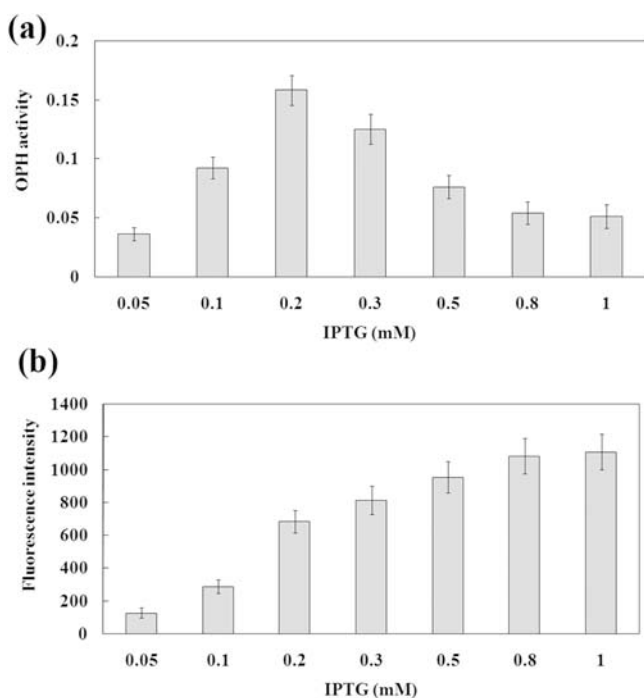


**Figure 2.** Whole-cell activity (a) and fluorescence (b) of *E. coli* carrying pPNC033 and pLMG18 under different levels of induction. The OPH activity was measured with parathion as the substrate. The data are mean values  $\pm$  standard deviations of three replicates.

**Stability of *E. coli* Codisplaying OPH and MPH–GFP Fusion.** Two major concerns in surface display are inhibition of cell growth and instability of the outer membrane.<sup>14,15</sup> To test whether surface display of OPH and MPH–GFP fusion inhibits cell growth, the growth kinetics of cells carrying pPNC033/pLMG18 or pVLT33/pUC18 were compared. No growth inhibition was observed for cells codisplaying OPH and MPH–GFP fusion. These cells carrying pPNC033/pLMG18 showed the same growth profile as those cells carrying pVLT33/pUC18. The two cultures reached the same final cell density after 48 h of incubation (Figure S1 in the Supporting Information). To monitor the stability of suspended cultures, whole-cell activity was determined each day over 2 weeks. The OP hydrolase activity of whole cells remained at essentially the original level over the 2 weeks (Figure S2 in the Supporting Information). These results show that codisplay of OPH and MPH–GFP fusion on the cell surface neither disturbs the outer membrane structure nor causes cell growth defects. Therefore, whole cells codisplaying OPH and MPH are very handy and stable in practical applications and can be recovered easily for repeated use. The stability of the cells observed here is in line with the results of previous studies in which the recombinant *E. coli* displaying OPH was also considerably more stable and robust than purified OPH, retaining 100% activity over a period of 1 month when maintained at 37 °C.<sup>9</sup>

**Degradation of OPs by Recombinant *E. coli*.** A mixture of paraoxon, parathion, methyl parathion, fenitrothion, diazinon, and chlorpyrifos was used to assess the degradation capability of the recombinant *E. coli*. As shown in Figure 3, all OPs (0.2 mM each) could be degraded completely by the recombinant strain carrying pPNC033/pLMG18 within 5 h. However, the concentration of OPs did not change in the uninoculated control. In contrast, only a few OPs could be degraded effectively by the recombinant strain carrying

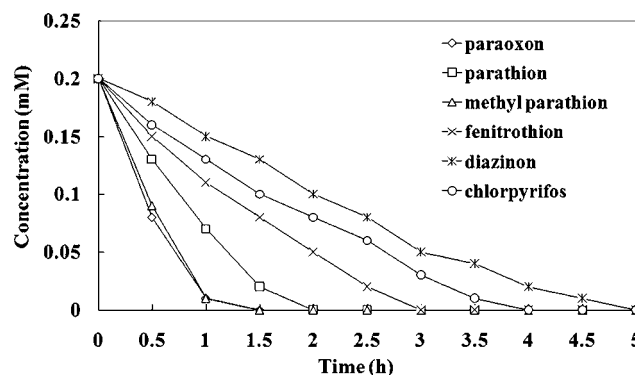


**Figure 3.** Degradation of a mixture of OPs by the recombinant *E. coli* carrying pPNC033 and pLMG18. Cell suspensions were incubated with a mixture containing six OPs (0.2 mM each) at 30 °C and 150 rpm. Samples were taken at different time points, and the residual concentration of OPs was measured by gas chromatography.

pPNC033 or pLMG18. These results indicate that the recombinant strain coexpressing OPH and MPH acquires an enlarged substrate range compared to strains expressing either the OPH and MPH and that it can be employed for the degradation of a mixture containing diethyl and dimethyl OPs. Because a variety of OPs usually coexist at a contaminated site, it is essential to create a recombinant strain with the broader substrate specificity. In this study, OPH and MPH were codisplayed on the cell surface of *E. coli*. The resulting strain has the ability to degrade a wide variety of OPs rapidly without the mass transport limitation.

**Potential of Recombinant *E. coli* for Use as a Whole-Cell Biosensor.** A number of pH-sensitive mutants have been generated, permitting GFP to be utilized as a pH indicator or to monitor exocytic/endocytic events as reflected by pH-induced changes in fluorescence.<sup>21,22</sup> It was reported that surface-displayed GFP was more sensitive to extracellular pH changes than GFP residing within the cell.<sup>32</sup> In this study, the fluorescence of the recombinant *E. coli* cells carrying pPNC033/pLMG18 at pH 6 dropped to 45% of that at pH 7.5 and was almost entirely quenched at pH 4. In contrast, the fluorescence of the control cells carrying pMG18 at pH 6 maintained 90% of that at pH 7.5. The GFP fluorescence was plotted versus the concentration of OPs, and the fluorescence intensity proportionally decreased with increasing concentrations of OPs. The linear relationship between the fluorescence and OPs concentration is shown in Figure S3 in the Supporting Information, with correlation coefficients  $R^2 = 0.9912$  and  $R^2 = 0.9938$ , respectively, for parathion and methyl parathion over a range of 0.02–0.2 mM. The low detection limit was 2  $\mu$ M. Because of the formation of protons during the hydrolysis of OPs and the sensitivity of GFP to the pH change, the GFP fluorescence can be used as an indicator for quantifying the concentration of OPs. Therefore, the recombinant *E. coli* could be used as a whole-cell biosensor for OPs detection by evaluating fluorescence changes as a function of OP concentrations.

Here, we demonstrated for the first time codisplay of OPH and MPH on the cell surface of *E. coli*. The recombinant *E. coli* showed a broader substrate range than recombinant *E. coli* with surface-displayed OPH.<sup>29</sup> Thus, the recombinant *E. coli* codisplaying OPH and MPH could be applied as a whole-cell biosensor for the detection of a wide range of OPs.

## ■ ASSOCIATED CONTENT

### Supporting Information

This material is available free of charge via the Internet at <http://pubs.acs.org>.

## ■ AUTHOR INFORMATION

### Corresponding Author

\*(P.X.) Phone/fax: 86-21-34206723. E-mail: pingxu@sjtu.edu.cn. (C.Q.) Phone: 86-10-64807191. Fax: 86-10-64807099. E-mail: qiaocl@ioz.ac.cn.

### Author Contributions

<sup>||</sup>R.L. and C.Y. contributed equally to this work.

### Funding

This study was financially supported by the National High Technology Research and Development Program of China (863 Program, No. 2013AA06A210), the Open Project of State Key Laboratory of Microbial Metabolism, Shanghai Jiao Tong University (No. MMLKF13-06), the Open Project of Tianjin Key Laboratory of Agro-environment and Agro-product Safety, Institute of Agro-Environmental Protection, Ministry of Agriculture (No. 2013-KF-06), and a Nankai University Youth Teacher Grant (No. 65012411).

### Notes

The authors declare no competing financial interest.

## ■ REFERENCES

- (1) Singh, B. K.; Walker, A. Microbial degradation of organophosphorus compounds. *FEMS Microbiol. Rev.* **2006**, *30*, 428–471.
- (2) Singh, B. K. Organophosphorus-degrading bacteria: ecology and industrial applications. *Nat. Rev. Microbiol.* **2009**, *7*, 156–164.
- (3) Mulbry, W. W.; Hams, J. F.; Kearney, P. C.; Nelson, J. O.; McDaniel, C. S.; Wild, J. R. Identification of a plasmid-borne parathion hydrolase gene from *Flavobacterium* sp. by Southern hybridization with *opd* from *Pseudomonas diminuta*. *Appl. Environ. Microbiol.* **1986**, *51*, 926–930.
- (4) Serdar, C. M.; Gibson, D. T. Enzymatic hydrolysis of organophosphates: cloning and expression of a parathion hydrolase gene from *Pseudomonas diminuta*. *Bio/Technology* **1985**, *3*, 567–571.
- (5) Sogorb, M. A.; Vilanova, E.; Carrera, V. Future application of phosphotriesterases in the prophylaxis and treatment of organophosphorus insecticide and nerve agent poisoning. *Toxicol. Lett.* **2004**, *151*, 219–233.
- (6) Cho, C. M.; Mulchandani, A.; Chen, W. Bacterial cell surface display of organophosphorus hydrolase for selective screening of improved hydrolysis of organophosphate nerve agents. *Appl. Environ. Microbiol.* **2002**, *68*, 2026–2030.
- (7) Cho, C. M.; Mulchandani, A.; Chen, W. Altering the substrate specificity of organophosphorus hydrolase for enhanced hydrolysis of chlorpyrifos. *Appl. Environ. Microbiol.* **2004**, *70*, 4681–4685.
- (8) Cui, Z.; Li, S.; Fu, G. Isolation of methyl parathion-degrading strain M6 and cloning of the methyl parathion hydrolase gene. *Appl. Environ. Microbiol.* **2001**, *67*, 4922–4925.
- (9) Richins, R. D.; Kaneva, I.; Mulchandani, A.; Chen, W. Biodegradation of organophosphorus pesticides by surface-expressed organophosphorus hydrolase. *Nat. Biotechnol.* **1997**, *15*, 984–987.
- (10) Shimazu, M.; Mulchandani, A.; Chen, W. Simultaneous degradation of organophosphorus pesticides and *p*-nitrophenol by a genetically engineered *Moraxella* sp. with surface-expressed organophosphorus hydrolase. *Biotechnol. Bioeng.* **2001**, *76*, 318–324.
- (11) Lei, Y.; Mulchandani, A.; Chen, W. Improved degradation of organophosphorus nerve agents and *p*-nitrophenol by *Pseudomonas putida* JS444 with surface-expressed organophosphorus hydrolase. *Biotechnol. Prog.* **2005**, *21*, 678–681.
- (12) Yang, C.; Cai, N.; Dong, M.; Jiang, H.; Li, J.; Qiao, C.; Mulchandani, A.; Chen, W. Surface display of MPH on *Pseudomonas putida* JS444 using ice nucleation protein and its application in detoxification of organophosphates. *Biotechnol. Bioeng.* **2008**, *99*, 30–37.
- (13) Takayama, K.; Suye, S.; Kuroda, K.; Ueda, M.; Kitaguchi, T.; Tsuchiyama, K.; Fukuda, T.; Chen, W.; Mulchandani, A. Surface display of organophosphorus hydrolase on *Saccharomyces cerevisiae*. *Biotechnol. Prog.* **2006**, *22*, 939–943.
- (14) Lee, S. Y.; Choi, J. H.; Xu, Z. Microbial cell-surface display. *Trends Biotechnol.* **2003**, *21*, 45–52.
- (15) Samuelson, P.; Gunneriusson, E.; Nygren, P. A.; Stahl, S. Display of proteins on bacteria. *J. Biotechnol.* **2002**, *96*, 129–154.
- (16) Earhart, C. F. Use of an Lpp-OmpA fusion vehicle for bacterial surface display. *Methods Enzymol.* **2000**, *326*, 506–516.
- (17) Kozloff, L. M.; Turner, M. A.; Arellano, F. Formation of bacterial membrane ice-nucleation lipoglycoprotein complexes. *J. Bacteriol.* **1991**, *173*, 6528–6536.
- (18) Wolber, P. K. Bacterial ice nucleation. *Adv. Microbiol. Physiol.* **1993**, *34*, 203–237.
- (19) Chalfie, M.; Tu, Y.; Euskirchen, G.; Ward, W. W.; Prasher, D. C. Green fluorescent protein as a marker for gene expression. *Science* **1994**, *263*, 802–805.
- (20) Gerdes, H.-H.; Kaether, C. Green fluorescent protein: applications to cell biology. *FEBS Lett.* **1996**, *389*, 44–47.
- (21) Kneen, M.; Farinas, J.; Li, Y.; Verkman, A. S. Green fluorescent protein as a noninvasive intracellular pH indicator. *Biophys. J.* **1998**, *74*, 1591–1599.
- (22) Patterson, G. H.; Knobel, S. M.; Sharif, W. D.; Kain, S. R.; Piston, D. W. Use of the green fluorescent protein and its mutants in quantitative fluorescence microscopy. *Biophys. J.* **1997**, *73*, 2782–2790.
- (23) Cormack, B. P.; Valdivia, R. H.; Falkow, S. FACS-optimized mutants of the green fluorescent protein (GFP). *Gene* **1996**, *173*, 33–38.
- (24) Sambrook, J.; Russel, D. W. *Molecular Cloning: A Laboratory Manual*, 3rd edn.; Cold Spring Harbor Laboratory Press: Cold Spring Harbor, NY, 2001.
- (25) de Lorenzo, V.; Eltis, L.; Kessler, B.; Timmis, K. N. Analysis of *Pseudomonas* gene products using *lacI<sup>q</sup>/Ptrp-lac* plasmids and transposons that confer conditional phenotypes. *Gene* **1993**, *123*, 17–24.
- (26) Liu, Z.; Yang, C.; Jiang, H.; Mulchandani, A.; Chen, W.; Qiao, C. Simultaneous degradation of organophosphates and 4-substituted phenols by *Stenotrophomonas* species LZ-1 with surface-displayed organophosphorus hydrolase. *J. Agric. Food Chem.* **2009**, *57*, 6171–6177.
- (27) Yang, C.; Liu, N.; Guo, X.; Qiao, C. Cloning of *mpd* gene from a chlorpyrifos-degrading bacterium and use of this strain in bioremediation of contaminated soil. *FEMS Microbiol. Lett.* **2006**, *265*, 118–125.
- (28) Li, L.; Kang, D. G.; Cha, H. J. Functional display of foreign protein on surface of *Escherichia coli* using N-terminal domain of ice nucleation protein. *Biotechnol. Bioeng.* **2004**, *85*, 214–221.
- (29) Yang, C.; Zhu, Y.; Yang, J.; Liu, Z.; Qiao, C.; Mulchandani, A.; Chen, W. Development of an autofluorescent whole-cell biocatalyst by displaying dual functional moieties on *Escherichia coli* cell surfaces and construction of a coculture with organophosphate-mineralizing activity. *Appl. Environ. Microbiol.* **2008**, *74*, 7733–7739.
- (30) Novick, R. P. Plasmid incompatibility. *Microbiol. Rev.* **1987**, *51*, 381–395.
- (31) Bokman, S. H.; Ward, W. W. Renaturation of *Aequorea* green fluorescent protein. *Biochem. Biophys. Res. Commun.* **1981**, *101*, 1372–1380.
- (32) Shi, H.; Su, W. W. Display of green fluorescent protein on *Escherichia coli* cell surface. *Enzyme Microb. Technol.* **2001**, *28*, 25–34.
- (33) Lan, W.; Gu, J.; Zhang, J.; Shen, B.; Jiang, H.; Mulchandani, A.; Chen, W.; Qiao, C. Coexpression of two detoxifying pesticide-degrading enzymes in a genetically engineered bacterium. *Int. Biodeterior. Biodegrad.* **2006**, *58*, 70–76.
- (34) Tomlin, C. *The Pesticide Manual*, 13th ed.; BCPC Publications: Hampshire, UK, 2003.

(35) Horne, I.; Sutherland, T. D.; Harcourt, R. L.; Russell, R. J.; Oakeshott, J. G. Identification of an *opd* (organophosphate degradation) gene in an *Agrobacterium* isolate. *Appl. Environ. Microbiol.* **2002**, *68*, 3371–3376.

(36) Rodrigue, A.; Chanal, A.; Beck, K.; Muller, M.; Wu, L. Co-translocation of a periplasmic enzyme complex by a hitchhiker mechanism through the bacterial Tat pathway. *J. Biol. Chem.* **1999**, *274*, 13223–13228.